Optimization of Packaging for PIN Photodiode Modules for 100Gbit/s Ethernet Applications

Jiang, Chenhui; Johansen, Tom Keinicke; Krozer, Viktor; Mekonnen, G. G.; Bach, H-G.

Published in:
Proceedings of 2007 Asia-Pacific Microwave Conference

Link to article, DOI:
10.1109/APMC.2007.4554950

Publication date:
2007

Document Version
Publisher's PDF, also known as Version of record

Citation (APA):
Jiang, C., Johansen, T. K., Krozer, V., Mekonnen, G. G., & Bach, H-G. (2007). Optimization of Packaging for PIN Photodiode Modules for 100Gbit/s Ethernet Applications. In Proceedings of 2007 Asia-Pacific Microwave Conference (pp. 623-626). Bangkok Thailand: IEEE. DOI: 10.1109/APMC.2007.4554950

Proceedings of Asia-Pacific Microwave Conference 2007

Optimization of Packaging for PIN Photodiode Modules for 100Gbit/s Ethernet Applications

C. Jiang[1], T. K. Johansen[1], V. Krozer[1], G. G. Mekonnen[2] and H-G. Bach[2]
[1]ElectroScience·Oersted, Technical University of Denmark, Lyngby, Denmark
cj@oersted.dtu.dk
[2]Fraunhofer Institute for Telecommunications, Heinrich-Hertz-Institut (HHI)
Einsteinufer 37, D-10587 Berlin, Germany
mekonnen@hhi.fhg.de

Abstract—**In this paper the packaging of optical components is investigated employing a conductor backed coplanar waveguide (CBCPW). The study is performed using 3D electromagnetic (EM) simulations in a broadband range up to 110GHz. Higher-order resonances are observed in both measurement and simulation results. Based on the verified EM simulation setup, the origin of resonances is identified and remedies are suggested in the paper. Several optimization schemes for achieving good transmission characteristics for the planar structure as well as for the coax-CPW transition are proposed such as properly coating side metallization on the CPW, substrate spacing to the metal housing, and developing metal posts in the substrate of the CPW.**

Index Terms-Coplanar waveguides, electromagnetic simulation, higher order resonances, waveguide transitions

I. INTRODUCTION

High speed multi-gigabit networks are demanded for very large volume information transmission in the future. 100Gbit/s Ethernet is considered to be the preferable next generation network after 10Gbit/s applications because of its higher speed and lower power consumption than 40Gbit/s proposal [1]. Designing of very high speed opto-electronic transceivers suitable for 100Gbit/s Ethernet is essential for developing such network system.

One of challenges for developing high-speed components aiming at 100Gbit/s Ethernet is the design of suitable packaging and interconnects. Higher-order mode propagations and resonances and the parasitics of transmission lines seriously degrade the performance of the packaging and interconnects at high frequency up to 110GHz. 3D electromagnetic (EM) simulation is a powerful tool for designing and optimizing the packaging and interconnects. The unwanted mode propagations and resonances can be studied and eliminated based on the simulations. The use of 3D EM simulation software is necessary due to the inherent 3D geometry, especially for an efficient coax-CPW transition. All the simulations in this paper have been accomplished with Ansoft HFSS v10.

In the following sections, a conductor backed coplanar waveguide (CBCPW) device is first investigated to validate the EM simulation for passive structures in the broadband range and to verify the excitation de-embedding procedures. Higher order resonances of the structure are investigated and explained theoretically. Based on the verified EM simulation setup, coplanar waveguide (CPW) to coaxial connector transitions in a pin photodiode (PD) module packaging for 100Gbit/s Ethernet applications are investigated and optimized.

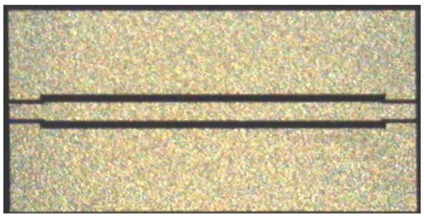

Figure 1. The CBCPW device under investigation

II. CONDUCTOR BACKED COPLANAR WAVEGUIDES

The CBCPW structure under investigation is shown in Fig. 1. The material of the substrate is quartz, and the metal is gold. The device is 4mm long. The characteristic impedance of the device is designed to be 50Ω. It is measured by a vector network analyzer with GSG probes. This measurement setup has been resembled in HFSS by using lumped ports to excite the device. Wave ports can not be used to excite such a device because the top side ground planes can be artificially connected to the backside ground plane by the edges of the wave ports.

The comparison between measured and simulated S_{21} for the structure in Fig.1 is shown in Fig. 2. The simulation results use a dielectric constant of 3.4 exploiting L-2L method [2] to remove the parasitics introduced by the lumped port excitation scheme. The calibrated simulation results fit the measurement results very well. The low frequency notch in the measured magnitude of S_{21} comes from measurement error and is ignored. This proves the validation of the EM simulation for passive structures in the broadband range up to 110GHz.

The magnitude of S_{21} has a notch around 90GHz and decays very fast beyond 100GHz as shown in Fig. 2 (a). The E-fields in the middle of substrate at 90GHz and 110GHz are shown in Fig. 3 (a) and (b), respectively. Both figures demonstrate strong E-field existing in the substrate under the top side ground planes. In this case, most of the EM energy is stored in the parallel plate configuration composed of parallel ground planes. A quasi-parallel plate mode is observed at the

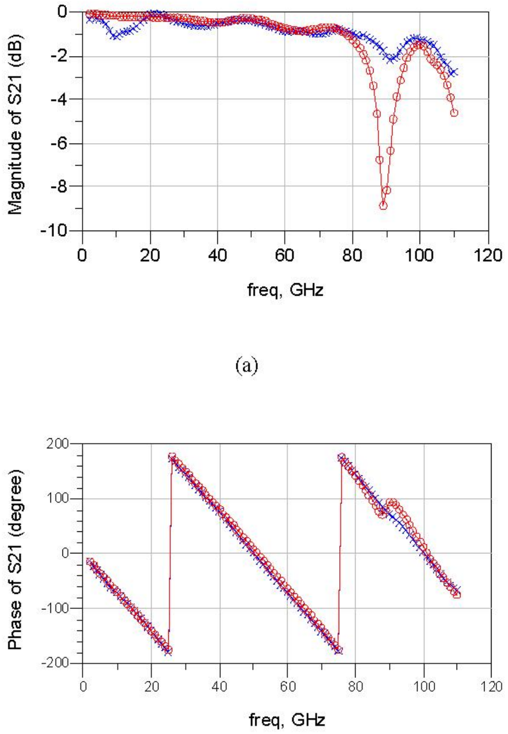

(a)

(b)

Figure 2. Comparison between measurment (-×-) and simulation (-o-) results: (a) magnitude of S_{21} (dB); (b) phase of S_{21} (degree);

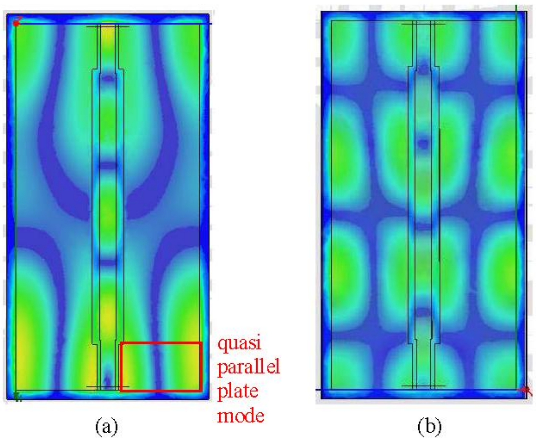

(a) (b)

Figure 3. E-field in the middle of the substrate at (a) 90GHz, (b) 110GHz

ends of the device in the E-field pattern at 90GHz as indicated in Fig.3 (a). The resonance frequency can be estimated by the following equation:

$$f_n = \frac{c}{2\sqrt{\varepsilon_r}} \bullet \frac{n}{d} \qquad (1)$$

where c is the velocity of the light in vacuum, ε_r is permittivity of the substrate, n is the index of the mode order and d is the length along the orientation of the resonance.

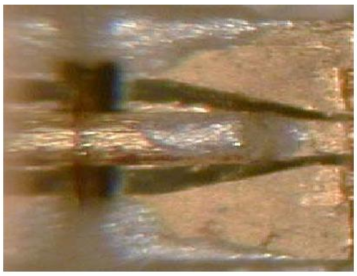

Figure 4. The CPW to coaxial connector transition in pin PD module.

The E-field pattern at 110GHz exhibits a typical patch antenna mode [3]. The resonance frequencies resulted from this mode can be calculated by

$$f_{mn} = \frac{c}{2\sqrt{\varepsilon_r}}\left[\left(\frac{m}{w}\right)^2 + \left(\frac{n}{l}\right)^2\right]^{0.5} \qquad (2)$$

where w and l are the width and the length of the equivalent patch antenna, m and n are the index of the mode order. Most of EM energy is radiated because of the antenna mode.

III. CPW TO COAXIAL CONNECTOR TRANSITIONS

The photoreceivers for 100Gbit/s applications are assembled using photodiode (PD) modules with fibre pigtail and a 1mm connector. CPW is used for the detector chip. CPW to coaxial connector transitions are the major waveguide discontinuities in the pin photodiode module packaging. The transition seriously affects the transmission property of the packaging, and it should be carefully designed and optimized.

A. *Coaxial Connnectors*

Agilent 11923A (1mm coax connectors) is a good candidate for CPW-coax transition. The connector is designed for high frequency (up to 110GHz) coaxial signal transmission into a microstrip (MS) or CPW waveguides [4]. The diameter of the launch pin is 162um, and the inside diameter of launch body feedthru is 380 um. The coaxial launch body has the cutoff frequency of the TE_{11} mode of about 360GHz [5]. It is much higher than the frequency range of interest here.

B. *CPW to Coaxial Connector Transitions with Side Matellization on the CPW*

3D EM simulation setup for CPW to coax connector transition is shown in Fig 5. A lumped port is used to excite the CPW side of the transition, and a wave port is used to excite the connector side of the transition, which is not shown in the figure. The substrate material is standard quartz with ε_r being 3.8. The length of the tapered CPW line is 600um. The side metallization along the orientation of the CPW is exploited to connect top ground planes with the backside ground plane. It is proven by EM simulation that the low frequency transmission characteristic is very poor when top ground planes are not connected to the backside ground plane. The gap between CPW and connector shown in Fig. 5 could influence the potential resonance in the transition.

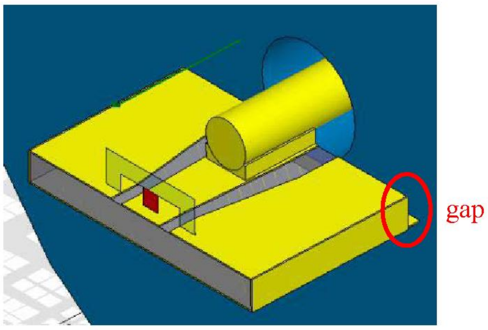

Figure 5. The EM simulation setup for the CPW to coaxial connector transition

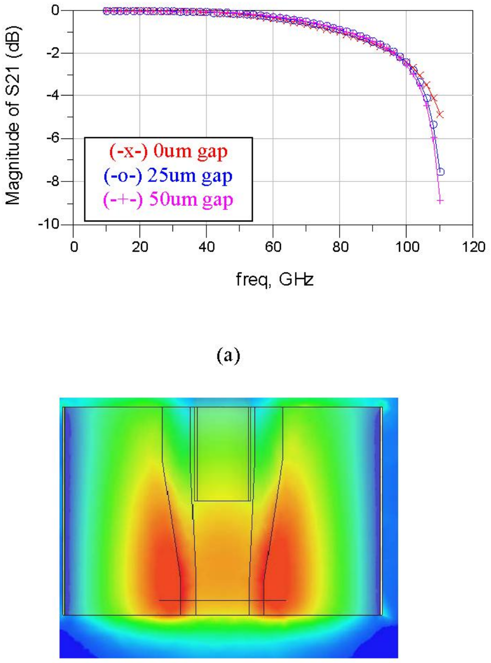

(a)

(b)

Figure 6. EM simulation on the CPW to connector transition, where the CPW has side metallization: (a) magnitude of S_{21} from CPW to connector with a variation of the gap; (b) E-field in the substrate at 110GHz with the gap being 50um.

The simulation results of the CPW to connector transition are shown in Fig. 6. All the magnitudes of S_{21} with different gaps decrease very fast over 100GHz. The E-field in the substrate at 110GHz with the gap being 50um is shown in Fig. 6 (b). A strong resonance field in the substrate is excited around the excitation scheme. The field exhibits quasi-parallel plate mode with a quarter wavelength perpendicular to the orientation of the CPW. This resonance degrades the high frequency transmission performance through the transition. It has to be eliminated by optimizing the transition.

In the first optimization scheme, called *case1*, only one longitudinal end of the CPW is coated with side metallization.

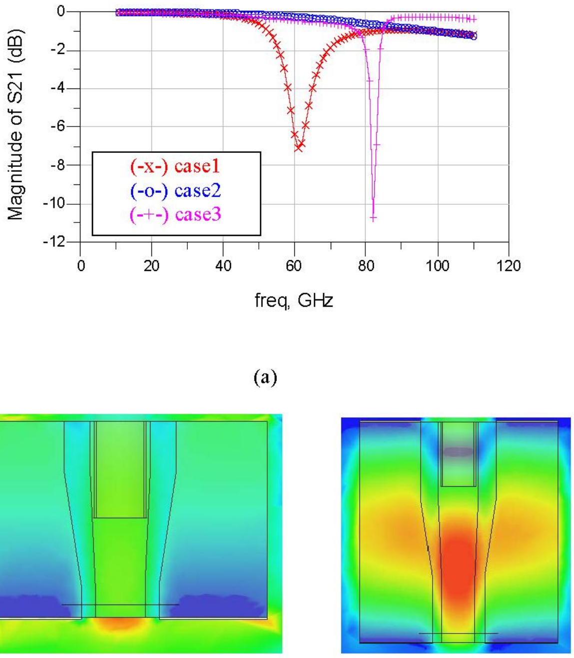

(a)

(b)

(c)

Figure 7. (a) magnitude of S_{21} from CPW to connector with different side metallization; case1 (-x-): only one side metallization is applied at the end of the 600um long CPW line; case2 (-o-): both ends of the 600um long CPW line are covered by metallization; case3 (-+-): both ends of the 1mm long CPW line are covered by metallization; (b) E-field in the substrate at resonance frequency for case1; (c) E-field in the substrate at resonance frequency for case3;

This optimization increases the high frequency transmission property, but a new resonance is introduced as shown in Fig. 7 (a). The E-field in the substrate at the resonance frequency, which is shown in Fig. 7 (b), demonstrates parallel plate mode having quarter wavelength, because one end is short and the other is open, which is similar to Fig. 6 (b) except for the orientation. When both ends of the CPW are covered by side metallization, which is called *case2*, the resonance is eliminated. However, if the CPW is extended to 1mm, which is called *case3*, a new resonance is observed in Fig. 7 (a). The corresponding E-field at the resonance frequency, which is shown in Fig. 7 (c), also exhibits parallel plate mode. It is half wavelength long with two zeros because both ends of the parallel plate are shorted. Both above resonance frequencies can be estimated using (1). The index numbers of resonance are 0.5 and 1 for quarter and half wavelength, respectively.

After investigating the transitions with different side metallization schemes, we conclude that the longitudinal side metallization is not suitable for high performance transmission in very high frequency range. The side metallization at both ends of the CPW effectively achieves good transmission property for the broadband requirement. However, this solution is only valid for the short CPW.

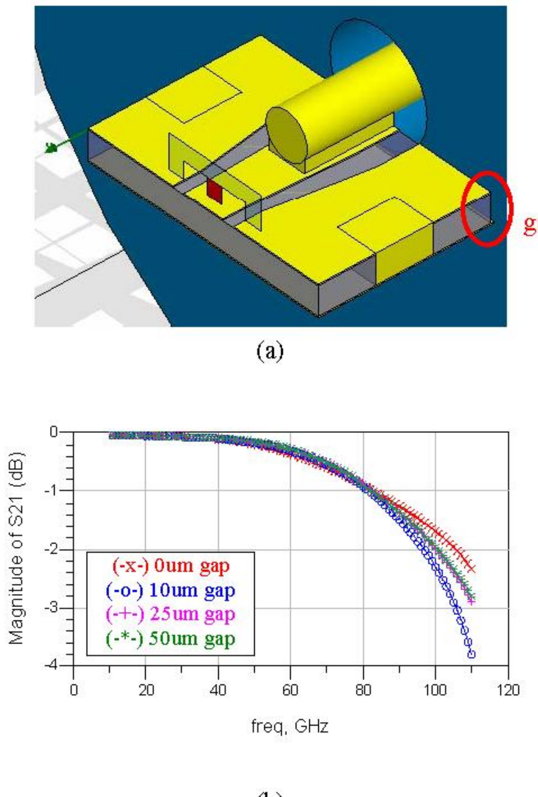

(a)

(b)

Figure 8. (a) The CPW line modified by inserting two metal posts in the substrate; (b) Magnitude of S_{21} for the CPW to connector transition with metal posts in the substrate of CPW line;

C. *Optimizing the Transition Using Metal Posts*

Another solution is provided by inserting two metal posts in the substrate. The solution is illustrated in Fig. 8 (a). The posts connect top and backside ground planes to obtain excellent transmission property in low frequency range. The size and the location of the post should be optimized. It has to be sufficiently large to eliminate higher order modes of resonance. However, being too large, they will influence the characteristic impedance of the CPW line, which is critical for the matching purposes. Posts should be located in the middle of line's edge to keep the potential resonance far away from the concerned band.

Fig. 8 (b) shows the simulated S_{21} with different gaps between the CPW and the coaxial connector as indicated in Fig 8 (a). Flat transmission properties are achieved by exploiting metal posts in the substrate. When the gap is zero, the transmission property is the best. It is because the least impedance mismatch exists in this case. When the gap is small as shown being 10um, the transmission property is worst in high frequency range. It is due to the strong E-field existing in the gap because of the tight coupling between the CPW and the connector due to the small gap. When the gap is larger than 25um, the gap does not influence the transmission property too much.

IV. CONCLUSION

In this paper, packaging aspects of photoreceivers operating up to 100 GHz have been studied theoretically and experimentally. The theoretical studies included long CBCPW structures. Higher order resonances have been observed both in simulation and measurement results. The validation of the EM simulation setup for the passive structure in broadband range has been verified by achieving good agreement between measured and simulated S-parameters of the device.

Based on the verified EM simulation setup, the CPW to coaxial connector transition for the pin PD module package has been investigated and optimized. Different schemes for coating the side metallization on the CPW have been analyzed, and the origin of potential resonances has been identified. Finally, a metal post optimization scheme is proposed to effectively achieve excellent broadband performance of the packaged module.

ACKNOWLEDGMENT

The authors would like to thank the European Commision for support under the 6th framework programme to the project "Opto-electronic integration for 100 Gigabit Ethernet Optical Networks (GIBON)".

REFERENCES

[1] "Next-generation 100-Gigabit Metro Ethernet (100 GbME) using multiwavelength optical ring" a. Zapata & al, J. Lightwave Technology, 22, 2004, pp 2420-2434.

[2] T. K. Johansen, C. Jiang, D. Hadziabdic, V. Krozer, "EM Simulation Accuracy Enhancement for Broadband Modeling of On-Wafer Passive Components", accepted, *EuMIC2007 Munich*, Oct. 2007

[3] J.A. Navarro and K. Chang, "Active microstrip antennas," in *Advances in Microstrip and Printed Antennas,* K.F.Lee and W.Chen, Eds. New York: Wiley, 1997, ch8

[4] Agilent Technology, "11923A Launch Assembly Operating and Service Manual", 2005

[5] David M. Pozer, Microwave Engineering, 2nd Edition, John Wiley & Sons, Inc. 1998